

Trihalomethyl Cations and Their Superelectrophilic Activation¹

George A. Olah,^{*,†} Golam Rasul,[†] Andrei K. Yudin,[†] Arwed Burrichter,[†]
G. K. Surya Prakash,^{*,†} A. L. Chistyakov,[‡] I. V. Stankevich,[‡] I. S. Akhrem,[‡]
N. P. Gambaryan,[‡] and M. E. Vol'pin[‡]

Contribution from the Donald P. and Katherine B. Loker Hydrocarbon Research Institute and Department of Chemistry, University of Southern California, University Park, Los Angeles, California 90089-1661, and Institute of Organoelement Compounds, Russian Academy of Science, 28 Vavilov Street, Moscow, Russia 117813

Received July 20, 1995. Revised Manuscript Received November 17, 1995[®]

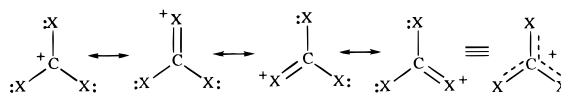
Abstract: *Ab initio* molecular orbital and density functional theory (DFT) calculations were performed to investigate energies, geometries, and reactivities of halomethyl cations and their protonated analogues. On the basis of calculated energies the observed superelectrophilic activation of the halomethyl cations in superacid solutions is discussed. The protonated halomethyl cations have considerable kinetic and thermodynamic stability. ¹³C NMR chemical shifts of selected systems were calculated by IGLO method and compared with experimental data.

Introduction

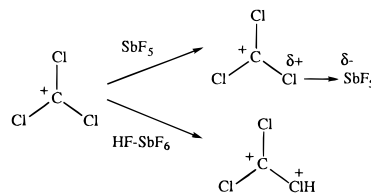
Whereas the highly electron deficient free methyl cation CH₃⁺ is not observable in solution chemistry, its alkyl- or halogen substituted analogues, such as (CH₃)₂CH⁺, (CH₃)₃C⁺, (CH₃)₂CX⁺, CH₃CX₂⁺, and CX₃⁺ (X = Cl, Br, I), have been prepared and studied as stable ions in superacid media. Trihalomethyl cations CX₃⁺ owe their thermodynamic stability² to the efficient p–p interaction between the positively charged carbon atom and the nonbonded electron pairs on the adjacent halogens (Scheme 1). The order of the charge-stabilizing effect of halogens was found to be Cl > Br > I. This order is in agreement with the relative increase in the size of the halogen atomic orbitals from chlorine to iodine leading to the least efficient overlap between positively charged carbon and iodine.³ If the halogen atoms of these ions were affected by further protolytic (or electrophilic) interaction, the electron deficiency of the corresponding carbocationic centers would become more pronounced, which should result in enhanced superelectrophilic reactivity (Scheme 2).⁴

In the early 1950s Willard et al.⁵ showed that CCl₄ readily exchanged chlorine atoms with ³⁶Cl labeled AlCl₃ even at –20 °C thus indicating ionization to CCl₃⁺. The trichloromethyl cation itself should not be a highly reactive electrophile based on the resonance effect of the three chlorine atoms. It is now suggested that the observed reactivity could be best explained by superelectrophilic activation. Later Bach et al.⁶ found that CCl₄/AlCl₃ is an extremely reactive hydride abstracting and ionic chlorinating system for adamantane. Similarly, use of CCl₄/HF-SbF₅ system (and related superacids) also greatly enhanced the reactivity of hydride abstraction from hydrocarbons to form carbocations as shown by Sunko et al.⁷ The reactivity of

Scheme 1



Scheme 2



halomethyl cations in superacid media was studied by several groups. Sommer et al.⁸ reported the increased reactivity of chloromethyl cations in hydride abstraction reactions with hydrocarbons in superacid media. They found that the reactivity decreased in the order CCl₃⁺ > CHCl₂⁺ ≫ CH₂Cl⁺. This was not expected because the stability of chloromethyl cations decreases in the same order since the number of 3p-donating chlorine atoms decreases. On these grounds CCl₃⁺ should be the least reactive species in the series. In order to explain this unusual behavior, protosolvation⁴ of the chlorine atoms in superacid was suggested. Protosolvation should enhance the electrophilic character of carbon in the corresponding halomethyl ion leading to the higher reactivity in the hydride-abstraction (Scheme 2). Therefore, as the number of halogen substituents increases, the electrophilicity should also augment.

In related studies Vol'pin et al.^{9a} found that polyhalomethanes in the presence of excess of AlBr₃ or AlCl₃ exhibit the properties of aprotic superacids. For example, CBr₄·2AlBr₃, CHBr₃·2AlBr₃, CCl₄·2AlBr₃, and CHCl₃·2AlBr₃ systems at 0–20 °C produce superelectrophiles which catalyze efficiently cracking, isomerization, and oligomerization of alkanes and cycloalkanes. The boron analogue for CCl₃⁺ is BCl₃; donor–acceptor complexation of BCl₃ with strong Lewis acids produces a superelectrophilic analogue.^{9b} This process is involved in the

[†] University of Southern California.

[‡] Russian Academy of Science.

[®] Abstract published in *Advance ACS Abstracts*, February 1, 1996.

(1) Chemistry in Superacids. Part 21. For Part 20 see: Olah, G. A.; Rasul, G.; York, C.; Prakash, G. K. S. *J. Am. Chem. Soc.* **1995**, *117*, 11211.

(2) Olah, G. A.; Heiliger, L.; Prakash, G. K. S. *J. Am. Chem. Soc.* **1989**, *111*, 8020.

(3) Olah, G. A.; Mo, Y. K. In *Carbonium Ions*; Olah, G. A., Schleyer, P. v. R., Eds.; Wiley Interscience: New York, 1976; Vol. V, Chapter 36.

(4) Olah, G. A. *Angew. Chem., Int. Ed. Engl.* **1993**, *32*, 767.

(5) Wallace, C. H.; Willard, J. E. *J. Am. Chem. Soc.* **1950**, *72*, 5275.

(6) Bach, R. D.; Badger, R. C. *Synthesis* **1979**, 529.

(7) Vancik, H.; Percac, K.; Sunko, D. E. *J. Am. Chem. Soc.* **1990**, *112*, 7418.

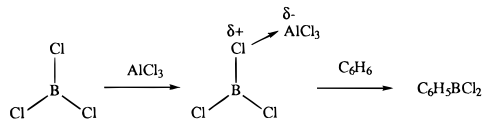
(8) Sommer, J.; Bukala, J. *Acc. Chem. Res.* **1993**, *26*, 370.

(9) (a) Vol'pin, M.; Akhrem, I.; Orlinkov, A., *New. J. Chem.*, **1989**, *13*, 771. (b) BCl₂⁺ has not yet been observed directly, but analogues with strong electron-donating groups such as N(CH₃)₂ as substituent were reported. Noth, H.; Staudigl, R. *Angew. Chem., Int. Ed. Engl.* **1981**, *20*, 794.

Table 1. Total Energies (–au), ZPE, and Relative Energies of Fluoro- and Chloromethyl Cations

no.	B3LYP/6-31G* (ZPE) ^a	relative energy ^b	MP2/6-31G* (ZPE) ^c	MP4(SDTQ)/MP2/6-31G*	relative energy ^d
1a	337.22630 (8.7)	0.0	336.43022 (8.6)	336.45792	0.0
1b	337.07358 (8.9)	96.0	336.27547 (8.8)	336.30374	96.5
1c	337.10816 (13.2)	78.6	336.30910 (13.1)	336.33905	79.1
2a	1418.32560 (5.2)	0.0	1416.46913 (5.3)	1416.52785	0.0
2b	1418.22942 (5.4)	60.6	1416.35794 (5.6)	1416.41762	69.5
2c	1418.32722 (9.8)	3.6	1416.46501 (10.0)	1416.52896	4.0
2d	1418.08389 (10.5)	157.0	1416.21631 (10.4)	1416.28145	159.7
2e	1418.12834 (14.1)	132.7	1416.26255 (14.1)	1416.33116	132.3
2f	1417.71337 (13.7)	392.7	1415.83619 (13.9)	1415.90687	398.3
2g	1417.72242 (15.9)	389.2	1415.84463 (16.2)	1415.91741	394.0
2h	957.45808 (4.2)	48.1	956.20782 (4.3)	956.25641	41.1
3a	956.72976 (10.6)	0.0	957.43821 (10.7)	957.48523	0.0
3b	958.62353 (10.9)	67.0	957.32167 (10.9)	957.36955	72.8
3c	958.71206 (15.2)	15.7	957.41711 (15.3)	957.46905	14.8
3d	958.448959 (15.8)	181.6	957.14494 (15.9)	957.19757	185.7
3e	958.47705 (19.2)	167.2	957.17340 (19.3)	957.22865	169.6
4a	499.11775 (15.3)	0.0	498.39395 (15.3)	498.42915	0.0
4b	498.99542 (15.6)	77.1	498.26132 (15.7)	498.29678	83.5
4c	499.06399 (20.0)	38.4	498.33388 (20.1)	498.37202	40.7

^a Zero point vibrational energies (ZPE) in kcal/mol at B3LYP/6-31G* level scaled by a factor of 0.96. ^b Relative energies based on B3LYP/6-31G*/B3LYP/6-31G* + ZPE. ^c ZPE at MP2/6-31G* level scaled by a factor of 0.93. ^d Relative energies based on MP4(SDTQ)/6-31G*/MP2/6-31G* + ZPE.

Scheme 3

Friedel–Crafts reaction of BCl_3 with arenes (Scheme 3) and explains the AlCl_3 catalyzed borination of benzene.^{9b} Whether an equilibrium $\text{BCl}_3 \cdot \text{AlCl}_3 \rightleftharpoons \text{BCl}_2^+ \text{AlCl}_4^-$ exists is of interest and the question of its relationship to isoelectronic CCl_2^{2+} will be discussed.

A theoretical investigation of the effects of protosolvation on the properties of halomethyl cations has never been done before. We now report on the *ab initio* and density functional theory (DFT)¹⁰ studies of halomethyl cations in order to investigate their electronic structure and properties. Our attention is focused mainly on the chloromethyl cations since their behavior in hydride abstraction is well documented. To probe the effects of protosolvation on the properties of chloromethyl cations we have calculated the mono-, di-, and triprotonated species as well as the transition states leading to them and compared the stabilities of the obtained ions with their corresponding progenitors. We also report the GIAO (gauge-including atomic orbital)-MP2¹¹ ¹³C NMR chemical shifts calculation on selected species.

Results and Discussion

Ab initio calculations were performed with the GAUSSIAN-94¹² package of programs. For X = F and Cl the geometry and frequency calculations were performed at the MP2/6-31G* level. Single point calculations at the MP4(SDTQ)/6-31G* level were performed on MP2/6-31G* optimized structures. Calculated energetics will be given at the MP4(SDTQ)/6-31G*/MP2-

6-31G* + ZPE (at MP2/6-31G*/MP2/6-31G* scaled by a factor of 0.93¹³) level, if not stated otherwise. For X = Br and I the geometry and frequency calculations were performed at the MP2/LANL2DZ (D95¹⁴ on C and H, Los Alamos ECP plus DZ¹⁵ on Br or I) level. Single point calculations at the MP4-(SDTQ)/LANL2DZ level were performed on MP2/LANL2DZ optimized structures. Calculated energetics will be given at the MP4(SDTQ)/LANL2DZ//MP2/LANL2DZ + ZPE (at MP2/LANL2DZ//MP2/LANL2DZ scaled by a factor of 0.96¹⁶) level, if not stated otherwise. For simplicity only the most stable isomers are reported.

Density functional theory (DFT) calculations were also performed with the GAUSSIAN-94 package of programs. For X = F and Cl the geometry and frequency calculations were performed at the B3LYP/6-31G* level and for X = Br and I at the B3LYP/LANL2DZ level. The total energies of the calculated structures are shown in Tables 1 and 2.

GIAO-MP2¹¹ ¹³C NMR chemical shift calculations have been performed with the ACES II program¹⁷ using the following basis sets:¹⁸ (1) triple- ζ polarization (tzp), C consisting of (10s 6p 1d/6s 3p 1d) contraction, d exponent 0.8; Cl consisting of (12s 9p 1d/7s 5p 1d) contraction, d exponent 0.65 and (2) double- ζ (dz), H consisting of (4s /2s) contraction.

Protonated Trifluoromethyl Cations. In the gas phase trifluoromethyl cation **1a** is stable and observed as an abundant species.¹⁹ However, in solution the great strength of C–F bond in CF_4 (140 kcal/mol) leads to rapid quenching of CF_3^+ even in low nucleophilicity fluorinated superacid media.² At MP2/6-31G* level, CF_3^+ was found to have a stable D_{3h} structure with a C–F bond length of 1.246 Å which is 0.084 Å shorter (Figure 1) than the C–F bond in CF_4 . This shortening is a result of efficient 2p–2p overlap between the nonbonded electron pairs on the fluorine atoms and adjacent positively charged carbon. Protonation of one of the fluorine atoms of

(10) Ziegler, T. *Chem. Rev.*, **1991**, *91*, 651.

(11) Gauss, J. *J. Chem. Phys. Lett.* **1992**, *191*, 614. Gauss, J. *J. Chem. Phys.* **1993**, *99*, 3629.

(12) Gaussian 94 (Revision A.1); Frisch, M. J.; Trucks, G. W.; Schlegel, H. B.; Gill, P. M. W.; Johnson, B. G.; Robb, M. A.; Cheeseman, J. R.; Keith, T. A.; Peterson, G. A.; Montgomery, J. A.; Raghavachari, K.; Al-Laham, M. A.; Zakrzewski, V. G.; Ortiz, J. V.; Foresman, J. B.; Cioslowski, J.; Stefanov, B. B.; Nanayakkara, A.; Challacombe, M.; Peng, C. Y.; Ayala, P. Y.; Chen, W.; Wong, M. W.; Andres, J. L.; Replogle, E. S.; Gomperts, R.; Martin, R. L.; Fox, D. J.; Binkley, J. S.; Defrees, D. J.; Baker, J.; Stewart, J. J. P.; Head-Gordon, M.; Gonzalez, C.; Pople, J. A. Gaussian, Inc.: Pittsburgh, PA, 1995.

(13) Sieber, S.; Buzek, P.; Schleyer, P. v. R.; Koch, W.; Carneiro, J. W. d. M.; *J. Am. Chem. Soc.* **1993**, *115*, 259.

(14) Dunning, T. H., Jr.; Hay, P. J. In *Modern Theoretical Chemistry*; Shaefer, H. F., Ed.; Plenum: New York, 1976; 1–28.

(15) Hay, P. J.; Wadt, W. R. *J. Chem. Phys.* **1985**, *82*, 270.

(16) Rauhut, G.; Pulay, P. *J. Chem. Phys.* **1995**, *99*, 3093.

(17) Stanton, J. F.; Gauss, J.; Watts, J. D.; Lauderdale, W.; Bartlett, R. J. *ACES II, an ab Initio Program System*; University of Florida: Gainesville, FL, 1991.

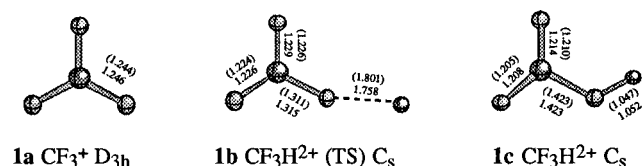
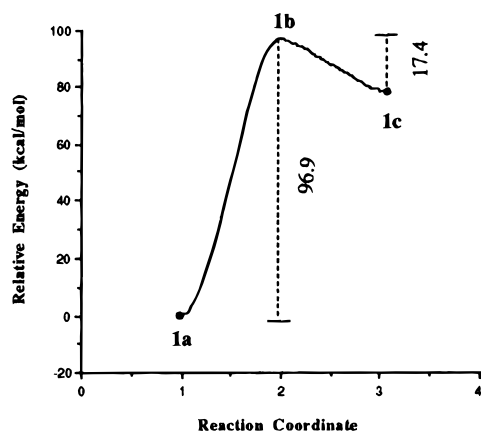
(18) Schafer, A.; Horn, H.; Ahlrichs, R. *J. Chem. Phys.* **1991**, *97*, 2571.

(19) Murdoch, H. D.; Weiss, E. *Helv. Chim. Acta* **1962**, *45*, 1927.

Table 2. Total Energies (–au), ZPE; and Relative Energies of Bromo- and Iodomethyl Cation

no.	B3LYP/LANL2DZ (ZPE) ^a	relative energy ^b	MP2/LANL2DZ (ZPE) ^c	MP4/LANL2DZ//MP2/LANL2DZ	relative energy ^d
5a	77.19574 (3.7)	10.3	76.42561 (3.6)	76.45260	15.5
5b	77.12580 (3.7)	55.4	76.32968 (3.7)	76.35905	74.3
5c	77.21991 (7.4)	0.0	76.44878 (7.4)	76.48330	0.0
5d	77.00843 (7.8)	133.1	76.23156 (7.8)	76.26773	136.7
5e	77.05672 (11.0)	106.0	76.29012 (11.0)	76.07069	99.6
5f	76.69181 (10.9)	334.9	75.91149 (11.1)	75.95584	334.7
5g	76.70395 (13.1)	329.5	75.92438 (13.3)	75.97121	327.2
6a	71.88885 (3.1)	38.4	71.13513 (3.1)	71.15963	44.7
6c	71.95598 (6.8)	0.0	71.20518 (6.8)	71.23670	0.0
6d	71.78151 (6.9)	68.1	71.01844 (7.0)	71.05335	115.3
6e	71.85326 (10.4)	109.6	71.10838 (10.3)	71.14640	60.2
6f	71.53791 (10.5)	247.2	70.77671 (10.6)	70.82027	265.1
6g	71.57245 (13.3)	266.0	70.81523 (13.5)	70.86219	241.7

^a Zero point vibrational energies (ZPE) in kcal/mol at B3LYP/LANL2DZ level scaled by a factor of 0.96. ^b Relative energies based on B3LYP/LANL2DZ //B3LYP/LANL2DZ + ZPE. ^c ZPE at MP2/LANL2DZ level scaled by a factor of 0.93. ^d Relative energies based on MP4(SDTQ)/LANL2DZ //MP2/LANL2DZ + ZPE.

**Figure 1.** MP2/6-31G* optimized (DFT B3LYP/6-31G*) geometries of **1a–c**.**Figure 2.** Calculated energetics of protonated CF_3^+ .

1a results in the dication CF_3H^{2+} (**1c**) which lies 79.1 kcal/mol (DFT 78.6 kcal/mol) higher than **1a** on the potential energy surface. The calculated kinetic barrier for the protonation of **1a** is 96.9 kcal/mol (Figure 2). The C_s symmetrical structure **1b** was found to be a transition state for the protonation. The 17.4 kcal/mol barrier for the deprotonation indicates that once formed, **1c** should be kinetically stable. As a direct consequence of the charge repulsion between positive charges on carbon and protonated fluorine in **1c** a significant lengthening (0.177 Å) of the corresponding C–F bond in **1c** compared to **1a** occurs. At the same time the remaining two C–F bonds shorten by 0.032 and 0.036 Å due to the further delocalization of positive charge caused by the charge–charge repulsion. Similar to CF_3H^{2+} (**1c**) in the gas phase, a $\text{CF}_3\cdot\text{SbF}_5^+$ complex may be involved in Lewis superacid media. This also should result in subsequent rapid quenching leading to the formation of CF_4 . Diprotonated CF_3^+ is not a minimum at the MP2/6-31G* level. Upon optimization the $\text{CF}_3\text{H}_2^{3+}$ ion dissociated into **1c** and H^+ .

Mono-, Di-, and Triprotonated Trichloromethyl Cations.

At MP2/6-31G* level, trichloromethyl cation CCl_3^+ (**2a**) exists as a stable minimum with D_{3h} symmetry (Figure 3). The C–Cl bond length of 1.648 Å in **2a** is significantly shorter compared to the C–Cl bond in CCl_4 (1.766 Å). This is indicative of the

Table 3. GIAO-MP2 Calculated ^{13}C NMR Chemical Shifts of CCl_3^+ and Its Mono-, Di-, and Triprotonated Forms

cation	GIAO-MP2/tzp/dz// B3LYP/6-31G*	GIAO-MP2/tzp/dz// MP2/6-31G*	expt.
TMS	0.0	0.0	0.0
2a	255.2	249.9	236.0 ^a
2c	217.5	214.7	
2e	218.9	214.8	
2g	292.6	275.5	

^a Experimental chemical shift taken from ref 2.

positive charge in **2a** being delocalized among three chlorine atoms. The monoprotection of trichloromethyl cation, accompanied with a kinetic barrier of 69.5 kcal/mol (DFT 60.6 kcal/mol), yields the dication $\text{CCl}_3\text{H}^{2+}$ (**2c**) which is only 4.0 kcal/mol higher in energy than the trichloromethyl cation. Deprotonation of **2c** has a considerable kinetic barrier of 65.5 kcal/mol. There is a 0.061 Å elongation of the bond between carbon and the protonated chlorine in **2c** due to the repulsion between the two adjacent positive charges. The remaining two carbon–chlorine bonds shorten by 0.042 and 0.045 Å compared to the trichloromethyl cation as the positive charge on carbon atom is delocalized in the Cl–C–Cl framework.

Thermodynamically dissociation of $\text{CCl}_3\text{H}^{2+}$ **2c** into linear CCl_2^{2+} **2h** and HCl is 41.1 kcal/mol less favorable than the dissociation into CCl_3^+ (**2a**) and H^+ . The dication CCl_2^{2+} **2h**, isoelectronic and isostructural to BCl_2^+ and CS_2 , is characterized by a short C–Cl distance of 1.515 Å.

Further protonation gives the tripositive C_{2v} symmetrical $\text{CCl}_3\text{H}_2^{3+}$ (**2e**)²⁰ which is destabilized by 132.3 kcal/mol compared to the **2a**. $\text{CCl}_3\text{H}_2^{3+}$ is kinetically feasible since the energy barrier of 27.4 kcal/mol should be overcome for the deprotonation. At this point the positive charge on carbon is stabilized by the p–p interaction with only one chlorine atom as shown in Scheme 4. This delocalization accounts for the observed shortening of the bond to 1.575 Å between the carbocationic center and the remaining unprotonated chlorine atom.

Addition of the third proton should greatly diminish the stability of the species since no resonance stabilization could be found in $\text{CCl}_3\text{H}_3^{4+}$ (**2g**). Indeed, we found **2g** to be 261.7 kcal/mol higher in energy on the potential energy surface than $\text{CCl}_3\text{H}_2^{3+}$. Deprotonation of $\text{CCl}_3\text{H}_3^{4+}$ leading to **2e** is accompanied by only 4.3 (DFT 3.5) kcal/mol barrier in agreement with the absence of stabilizing p–p interactions in the triprotonated species (Figure 4). Therefore, the trication **2g** should be both thermodynamically and kinetically unstable.

We have also calculated the ^{13}C NMR chemical shifts of CCl_3^+ and its mono-, di-, and triprotonated forms by GIAO-

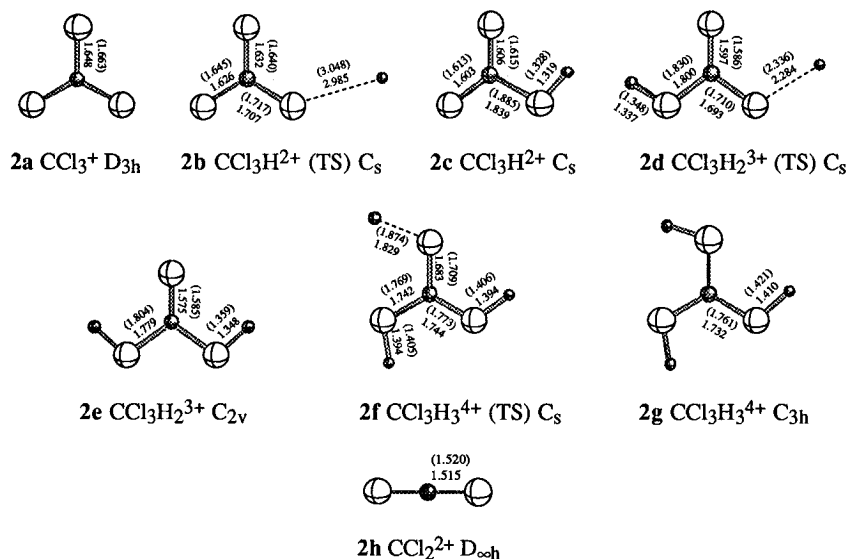


Figure 3. MP2/6-31G* optimized (DFT B3LYP/6-31G*) geometries of 2a–g.

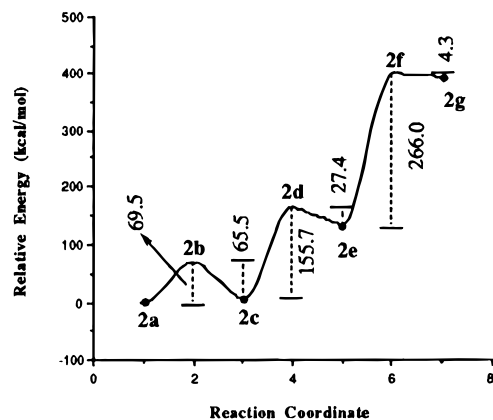
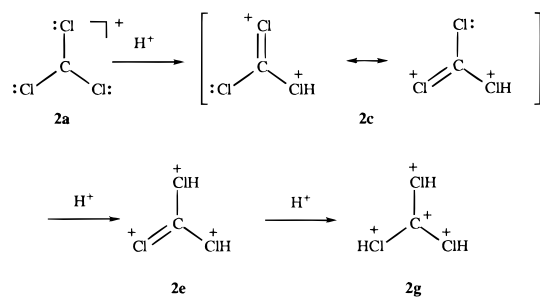


Figure 4. Calculated energetics of protonated CCl_3^+ .

Scheme 4



MP2¹¹ method using tzp/dz¹¹ basis set on MP2/6-31G* (and B3LYP/6-31G*) geometries (Table 3). The calculated $\delta^{13}\text{C}$ of CCl_3^+ (2a) is 249.9 compared with the experimental value of 236.0. Remarkably, the calculated $\delta^{13}\text{C}$ 214.7 of $\text{CCl}_3\text{H}^{2+}$ 2c and $\delta^{13}\text{C}$ 214.8 of $\text{CCl}_3\text{H}_2^{3+}$ 2e are both shielded by 35 ppm from the calculated $\delta^{13}\text{C}$ of CCl_3^+ (2a). However, the calculated $\delta^{13}\text{C}$ 275.5 of $\text{CCl}_3\text{H}_3^{4+}$ (2g) is 26.6 ppm deshielded from the $\delta^{13}\text{C}$ of CCl_3^+ (2a).

Mono- and Diprotonated Dichloromethyl Cations. At MP2/6-31G* dichloromethyl cation has a C_{2v} symmetrical structure 3a (Scheme 5). The C–Cl bond in 3a is 0.025 Å shorter than the corresponding bond in CCl_3^+ since positive charge is distributed between two chlorine atoms. This leads to a diminished overall stabilization (Figure 5). The global minimum for the monoprotonated dichloromethyl cation corresponds to the dication $\text{CHCl}_2\text{H}^{2+}$ (3c).

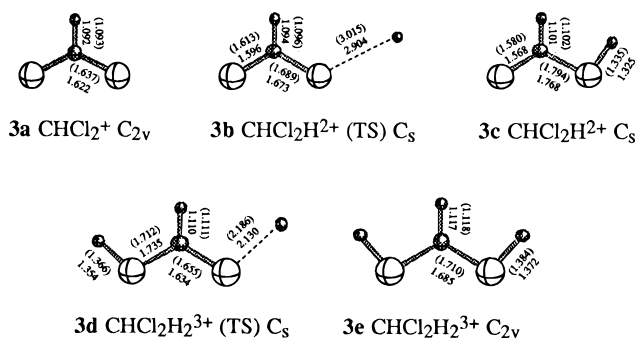
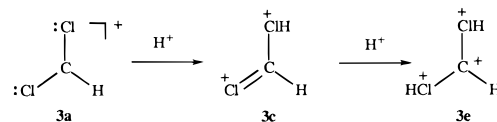
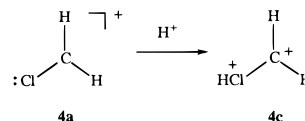


Figure 5. MP2/6-31G* optimized (DFT B3LYP/6-31G*) geometries of 3a–e.

Scheme 5



Scheme 6



The ion 3c is destabilized by 14.8 kcal/mol compared to 3a. As in the case of $\text{CCl}_3\text{H}_2^{3+}$ ion, the positive charge on the carbon atom in 3c could be stabilized by the p–p interaction with only one chlorine atom. This stabilization is reflected in the shortened C–Cl bond of 1.568 Å between the carbon atom and the remaining unprotonated chlorine. Kinetic barrier for the deprotonation of 3c is 58.0 kcal/mol which supports its kinetic stability. Further protonation gives the tripositive $\text{CHCl}_2\text{H}_2^{3+}$ cation (3e) with C_{2v} symmetry. The ion 3e possesses only 16.1 kcal/mol of kinetic stability (Figure 6) which is consistent with the absence of resonance stabilization.

The discussed results are for the idealized gas phase ions and might be different in the condensed state. Related electrophilic solvation (protolytic solvation) of the chlorine atoms by superacid media can account for superelectrophilic activation of reported reactions.

Monoprotonated Chloromethyl Cations. Monochloromethyl cation converged to a stable C_{2v} symmetrical structure.

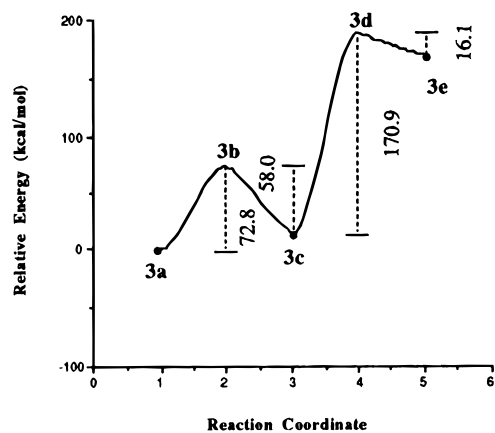


Figure 6. Calculated energetics of protonated HCCl_3^+ .

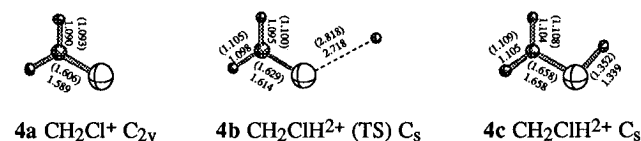


Figure 7. MP2/6-31G* optimized (DFT B3LYP/6-31G*) geometries of 4a–c.

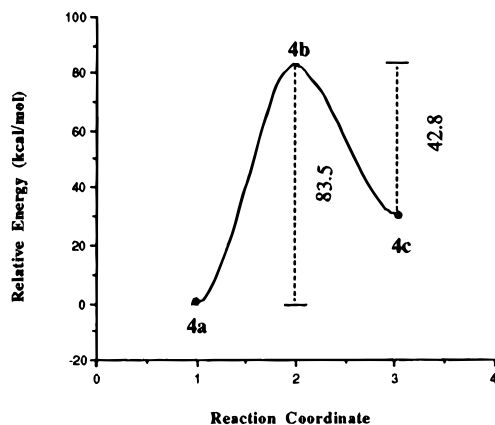


Figure 8. Calculated energetics of protonated CH_2Cl^+ .

Protonation of the chlorine atom accompanied with a kinetic barrier of 83.5 kcal/mol results in dipositive species $\text{CH}_2\text{ClH}_2^+$ (**4c**) (Scheme 6 and Figures 7 and 8). The ion $\text{CH}_2\text{ClH}_2^+$ (**4c**) lies 40.7 kcal/mol above CH_2Cl^+ (**4a**) on the potential energy surface.

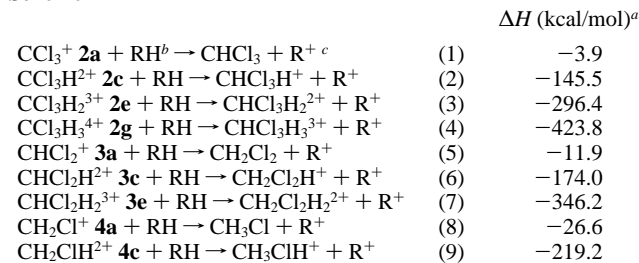
Comparison of the energy changes in the course of super-electrophilic activation of tri-, di-, and monochloromethyl cations shows that the decrease in the number of chlorine atoms attached to the carbocationic center lowers the kinetic and thermodynamic stability of the corresponding protonated species.

In order to further investigate the difference in thermodynamic stability among the chloromethyl cations we considered the isodesmic reactions 1–9 (Scheme 7). Isodesmic reaction is one of the major tools in theoretical investigation to probe subtle electronic effects in chemical structures. By definition, isodesmic reaction is a transformation in which the number of bonds of each type is conserved, while the relationship among the bonds is altered.²¹ Propane was selected as a hydride-donor. Reaction 1 is exothermic by only 3.9 kcal/mol. The similar process involving dichloromethyl cation (reaction 5) is ac-

(20) We searched for conformational minima for the rotation around C–X (H) bonds. We found other local minima that are not important for the topics discussed in this paper. The structures shown in the Figures are the calculated lowest energy forms.

(21) Hehre, W. J.; Radom, L.; Schleyer, P. v. R.; Pople, J. A. *Ab Initio Molecular Orbital Theory*; Wiley-Interscience: New York, 1986; p 226.

Scheme 7



^a MP4(SDTQ)/6-31G**//MP2-6-31G* + ZPE (MP2/6-31G**//MP2-6-31G*). ^b R = $\text{CH}_3\text{CH}_2\text{CH}_3$. ^c R⁺ = $\text{CH}_3\text{CH}^+\text{CH}_3$.

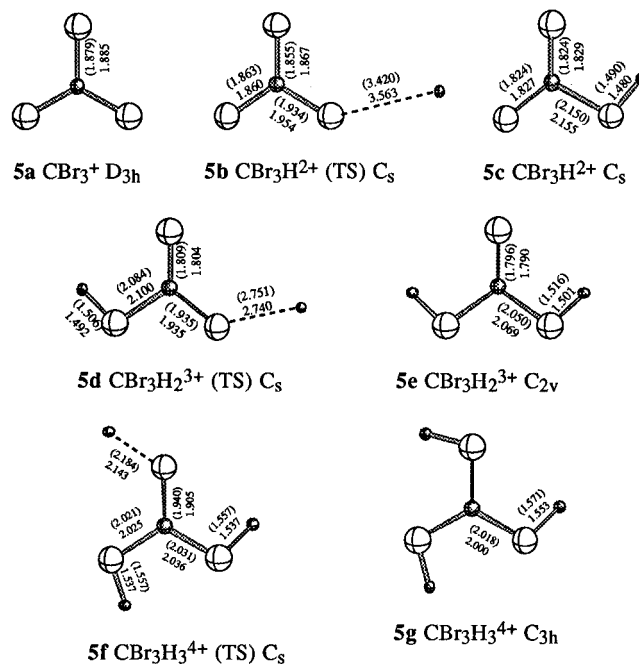


Figure 9. MP2/LANL2DZ optimized (DFT B3LYP/LANL2DZ) geometries of 5a–g.

companied by -11.9 kcal/mol enthalpy change. When monochloromethyl cation acts as a hydride-abstracting species, the reaction is exothermic by 26.6 kcal/mol. Comparison of the enthalpy changes indicates that CCl_3^+ is the most stable cation in the series which is in accordance with the high degree of positive charge stabilization by three chlorine atoms.

Clearly, from the calculated energetics for the reactions 1, 5, and 8 the relative thermodynamic stability of the free (unprotonated) chloromethyl cations follows the order CCl_3^+ (**2a**) (ΔH -3.9) > CHCl_2^+ (**3a**) (ΔH -11.9) > CH_2Cl^+ (**4a**) (ΔH -26.6). Protonation dramatically decreases the stability of the trichloromethyl cation. The reactions 2, 3, and 4 are exothermic by 145.5, 296.4, and 423.8 kcal/mol, respectively. Mono- and diprotonation also markedly decrease the stability of the dichloromethyl cation (reactions 6 and 7 are exothermic by 174.0 and 346.2 kcal/mol, respectively). Finally, monoprotonation also significantly decreases the stability of chloromethyl cation (reaction 9 is exothermic by 219.2 kcal/mol).

Mono-, Di-, and Triprotonated Tribromomethyl Cations. We have calculated CBr_3^+ **5a** and its mono- **5c**, di- **5e**, and triprotonated **5g** forms and the structures are depicted in Figure 9. The calculated protodissociation barriers for the CBr_3H_2^+ (**5c**), $\text{CBr}_3\text{H}_2^{3+}$ (**5e**), and $\text{CBr}_3\text{H}_3^{4+}$ (**5g**) are 74.3, 37.1, and 7.5 kcal/mol, respectively, indicating that the CBr_3H_2^+ (**5c**) and $\text{CBr}_3\text{H}_2^{3+}$ (**5e**) could be kinetically stable, whereas the $\text{CBr}_3\text{H}_3^{4+}$ (**5g**) is expected to be relatively unstable.

It is particularly interesting to note that monoprotonated CBr_3H_2^+ (**5c**) is 15.5 kcal/mol more stable than CBr_3^+ (**5a**).

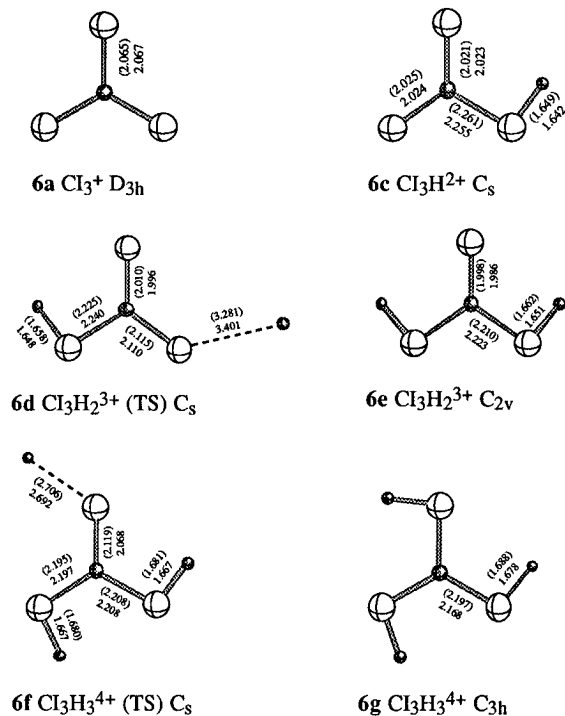


Figure 10. MP2/LANL2DZ optimized (DFT B3LYP/LANL2DZ) geometries of **6a–g**.

Again all the discussed results are for idealized gas phase and might be different in the condensed phase wherein electrophilic (protolytic) solvations would *de facto* be operative.

Mono-, Di-, and Triprotonated Triiodomethyl Cations. As expected, Cl_3H_2^+ (**6c**) is also 44.7 kcal/mol more stable than Cl_3^+ (**6a**) (compared to 15.5 kcal/mol for the bromo system). The calculated protodissociation barrier for the $\text{Cl}_3\text{H}_2^{3+}$ (**6e**) and $\text{Cl}_3\text{H}_3^{4+}$ (**6g**) are 55.1 and 23.4 kcal/mol, respectively, indicating that the $\text{Cl}_3\text{H}_2^{3+}$ (**6e**) and even $\text{Cl}_3\text{H}_3^{4+}$ (**6g**) will be kinetically stable. We could not find the transition state for the formation of Cl_3H_2^+ (**6c**) from Cl_3^+ (**6a**) and H^+ , probably due to a low energy barrier. The optimized geometries of the iodomethyl cations are given in Figure 10.

Overall the DFT methods generally give reliable geometries and energies compared to the high-level MP2 calculations as shown by data in Figures 1, 3, 5, 7, 8, and 9 and Tables 1 and 2. At the same time DFT methods are by far less time demanding which makes them a successful alternative to traditional methods for the calculations of molecular properties of charged species.

Whereas in our present study the emphasis was placed on the protolytic activation of halomethyl cations, Lewis acid induced activation of the halogen nonbonded electron pairs of the halomethyl cations such as those involving excess of aluminium trihalides also lead to such superelectrophilic activations.

It should be noted that all calculational data refer to isolated idealized gas phase. However, in the condensed phase electrophilic (protolytic) solvation or clustering effects may have great influence. In particular in small di-, tri-, and tetracations, such interactions should diminish the effect of charge–charge repulsion and thus could bring the cations into more thermodynamically feasible range.

Counterions have certainly important roles to play in the protonation equilibria. However, exceedingly delocalized and weak nucleophiles like SbF_6^- or related $\text{Sb}_2\text{F}_{11}^-$ might not compete efficiently with the rather localized lone pairs of the mono- or dications. If these anions were viable bases, the rate of reported proton/deuterium exchange of H_3O^+ in DF/SbF_5 should not be accelerated by an increase in the acidity of the solution.²² In our studies *de facto* protonated (or polyprotonated) halomethyl di(poly)cations were considered as model systems for superelectrophilic activation. Under experimental conditions of Bronsted or Lewis acid activated reactions the nonbond halogen electron pairs can be overall involved in donor–acceptor type interactions, i.e., electrophilic solvation.

The significance of the reported study lies in our better understanding of the superacid-induced reactions involving halomethyl cations. As was shown earlier,²³ consideration of the superelectrophilic activation offers an adequate explanation of the observed experimental data for a variety of superacid-catalyzed reactions. We have extended the principle of superelectrophilic activation to the halomethyl cations (wherein neighboring halogen participation is diminished) and have shown that reported experimental results are consistent with the proposed concept.

Acknowledgment. Support of our work by the National Science Foundation is gratefully acknowledged.

JA952408F

(22) Olah, G. A.; Prakash, G. K. S.; Barzaghi, M.; Lammertsma, K.; Schleyer, P. v. R.; Pople, J. A. *J. Am. Chem. Soc.* **1986**, *108*, 19032.

(23) Olah, G. A.; Rasul, G.; Aniszfeld, R.; Prakash, G. K. S. *J. Am. Chem. Soc.* **1992**, *114*, 5608. Weiske, T.; Koch, W.; Schwarz, H.; *J. Am. Chem. Soc.* **1993**, *115*, 6312. Hartz, N.; Golam, R.; Olah, G. A. *J. Am. Chem. Soc.* **1993**, *115*, 1277.